Survival of Trojan-Type Companions of Neptune During Primordial Planet Migration

Stephen J. Kortenkamp*,†, Renu Malhotra*, and Tatiana Michtchenko‡

ABSTRACT

We investigate the survivability of Trojan-type companions of Neptune during primordial radial migration of the giant planets Jupiter, Saturn, Uranus, and Neptune. We adopt the usual planet migration model in which the migration speed decreases exponentially with a characteristic time scale τ (the e-folding time). We perform a series of numerical simulations, each involving the migrating giant planets plus ∼1000 test particle Neptune Trojans with initial distributions of orbital eccentricity, inclination, and libration amplitude similar to those of the known jovian Trojans asteroids. We analyze these simulations to measure the survivability of Neptune's Trojans as a function of migration rate. We find that orbital migration with the characteristic time scale $\tau = 10^6$ years allows about 35% of pre-existing Neptune Trojans to survive to 5τ, by which time the giant planets have essentially reached their final orbits. In contrast, slower migration with $\tau = 10^7$ years yields only a ∼5% probability of Neptune Trojans surviving to a time of 5τ. Interestingly, we find that the loss of Neptune Trojans during planetary migration is not a random diffusion process. Rather, losses occur almost exclusively during discrete episodes when Trojan particles are swept by secondary resonances associated with mean-motion commensurabilities of Uranus with Neptune. These secondary resonances arise when the circulation frequencies, f, of critical arguments for Uranus-Neptune mean-motion near-resonances (e.g., $f^{\rm UN}_{1:2}$, $f^{\rm UN}_{4:7}$) are commensurate with harmonics of the libration frequency of the critical argument for the Neptune-Trojan 1:1 mean-motion resonance ($f^{\rm NT}_{1:1}$). Trojans trapped in the secondary resonances typically have their libration amplitudes amplified until they escape the 1:1 resonance with Neptune. Trojans with large libration amplitudes are susceptible to loss during sweeping by numerous high order secondary resonances (e.g., $f^{\rm UN}_{1:2} \approx 11 f^{\rm NT}_{1:1}$). However, for the slower migration, with $\tau = 10^7$ years, even tightly bound Neptune Trojans with libration amplitudes below 10° can be lost when they become trapped in 1:3 or 1:2 secondary resonances between $f^{\rm UN}_{1:2}$ and $f^{\rm NT}_{1:1}$. With $\tau = 10^7$ years the 1:2 secondary resonance was responsible for the single greatest episode of loss, ejecting nearly 75% of existing Neptune Trojans. This episode occurred during the late stages of planetary migration when the remnant planetesimal disk would have been largely dissipated. We speculate that if the number of bodies liberated during this event was sufficiently high they could have caused a spike in the impact rate throughout the solar system.

∗ University of Arizona, Tucson, AZ

† Planetary Science Institute, Tucson, AZ

‡ Universidade de São Paulo, São Paulo, Brasil

I. INTRODUCTION

Nearly 1500 asteroids are known to share Jupiter's orbit, locked in 1:1 mean-motion resonance with the giant planet. These so-called Trojan asteroids form two swarms in the Lagrange equilibrium regions leading (L_4) and trailing (L_5) Jupiter in its orbit by 60°. Only a single non-jovian Trojan-type companion is yet known in the outer solar system, minor planet 2001 QR322 in Neptune's trailing L_5 region (Chiang 2003; Marsden 2003). The lack of saturnian Trojans may be explained by the chaotic effects of resonances with other planets, which disrupt what would otherwise be stable Trojan regions (Holman & Wisdom 1993; de la Barre *et al.* 1996). Trojans of Uranus may also have been largely depleted by dynamical instabilities over the age of the solar system (Nesvorný & Dones 2002). The paucity of Neptune Trojans, however, is more puzzling. Most investigations into the stability of hypothetical Neptune Trojans (e.g., Weissman & Levison 1997; Nesvorný & Dones 2002) suggest that if a primordial population once existed then some sizable remnant (∼50%) of it should be preserved today. Prior to 2001 there had been no discoveries of Neptune Trojans, neither serendipitously nor in dedicated surveys (Chen *et al.* 1997). This fact was used to set crude limits on the size distribution of any existing population (Nesvorný & Dones 2002). However, these upper limits are weak, and do not preclude a population of Neptune Trojans that may exceed the population of Jupiter Trojans. Nevertheless, the current apparent scarcity of Neptune Trojans is interesting from a dynamical point of view. This, together with the orbital characteristics of 2001 QR322, may provide important clues to Neptune's origin and the primordial orbital evolution of the giant planets.

The early dynamical evolution of the outer solar system is thought to involve significant radial migration of the four giant planets (Fernández & Ip 1984, 1996; Hahn & Malhotra 1999). The cause of this migration is the planets' dynamical clearing of the residual planetesimal disk during the late stages of planet formation. Some clues that suggest past planetary migration include the existence of the Oort cloud of comets, orbital characteristics of plutinos and other resonant Kuiper belt objects (KBOs) trapped in mean-motion resonance with Neptune (Malhotra 1993, 1995; Chiang & Jordan 2002), the high inclination classical KBOs (Gomes 2003), and depletion of the outer asteroid belt (Liou & Malhotra 1997). Detailed descriptions of the migration process can be found in Fernández & Ip (1984, 1996) and Hahn & Malhotra (1999). Here we simply re-state the general scenario, highlighting the effects on Neptune's orbit.

In the beginning, Neptune is embedded in a planetesimal disk and we will assume it has a mean specific orbital angular momentum roughly equal to that of the planetesimals in its gravitational vicinity. Of those planetesimals encountered by Neptune about equal numbers will be scattered inward and outward, thus initially there is no net change in Neptune's orbital energy or angular momentum, so no migration of Neptune's orbit. Most planetesimals scattered outward eventually return to Neptune's region, with only minor losses from those receiving sufficient stellar perturbations to be boosted into the Oort cloud. These returning planetesimals can again be scattered by Neptune either inward or outward. Thus, most of the energy and angular momentum lost by Neptune to outward scattering can be recaptured upon return of the planetesimal. However, those planetesimals scattered inward by Neptune have the opportunity to encounter Uranus, Saturn, and Jupiter. Jupiter essentially controls the overall dynamics because it is very effective at ejecting planetesimals from the solar system. Planetesimals scattered inward by Neptune and subsequently

ejected by Jupiter cannot return for another encounter with Neptune (or Jupiter). Thus, Neptune retains the energy and angular momentum gained from them. In this scenario Jupiter provides more than the required energy and angular momentum to clear the remnant planetesimal disk, with the extra going toward expansion of Neptune's orbit. Jupiter thus migrates inward, though only slightly owing to its large mass. The early evolution of Saturn and Uranus are somewhat analogous to Neptune's, with each of these planets also migrating outward at Jupiter's expense.

Modeling of the cause and effects of planetary migration by planetesimal scattering (e.g., Hahn & Malhotra 1999; Gomes 1997) has yielded approximate semi-major axis migration distances, Δa, of -0.2, 0.8, 3.0, and 7.0 AU for Jupiter, Saturn, Uranus, and Neptune, respectively. The present semi-major axes of these planets are about 5.2, 9.5, 19.2, and 30.1 AU. Effective constraints on the early orbital evolution of the giant planets can be found in the orbital eccentricities of Pluto and other Kuiper belt objects trapped in 2:3 mean-motion resonance with Neptune. Using these constraints, Malhotra (1993, 1995) estimated that 5 AU should be considered a minimum migration distance for Neptune. Gomes (1997, 2000) and Malhotra (1998) suggested that a 9–10 AU migration might be necessary to account for the plutino inclinations. Constraints on the timescale of migration have come from the magnitude of Δa for Neptune (Hahn & Malhotra 1999), from relative populations of the 2:3 and 1:2 resonant KBOs (Malhotra 1995; Friedland 2000; Chiang & Jordan 2002), and plutino inclinations (Gomes 1997). With the discovery of 2001 QR 322, a new class of small body in resonance with Neptune has become available for study. Our aim with this paper is to begin examining the constraints such bodies may place on the early dynamical evolution of the giant planets.

The critical argument for a Trojan-type particle, an object in 1:1 mean-motion resonance with a planet, is given by $\phi_{1:1} = \lambda - \lambda_{\rm pln}$, where λ and $\lambda_{\rm pln}$ are the mean longitudes of the particle and planet. When a particle and planet are not in resonance $\phi_{1:1}$ circulates through all angles 0 to 360°. For a particle trapped in the planet's leading L_4 or trailing L_5 regions, $\phi_{1:1}$ librates about $+60°$ or $-60°$, respectively. The full magnitude of the difference between the extremal values of $\phi_{1:1}$ is called the libration amplitude. The time required for one complete libration of $\phi_{1:1}$ is the libration period. The effects of a planet's radial migration on the libration amplitude of a Trojan-type companion has been explored for the planar circular restricted three-body problem consisting of the sun, planet, and massless Trojan particle. Fleming and Hamilton (2000) derived the expression $A_f/A_i \propto (a_f/a_i)^{-1/4}$, where A is the Trojan libration amplitude, a is the planet's semi-major axis, and the subscripts denote the final and initial values. Inward radial migration increases A while outward migration decreases A. Numerical simulations by Fleming and Hamilton (2000) confirmed the validity of their expression for small initial libration amplitudes ($A_i < 30°$) and "slow" (adiabatic) migration. This single-planet model of Trojan stability during planetary migration is useful for demonstrating basic principles of the effects of migration. A straight forward application of this expression to our migration distances implies a slight decrease of about 5% in the libration amplitude of Neptune's Trojans. However, we show here that the gravitational perturbations of multiple migrating giant planets, especially at resonance crossings, have a profound effect on Trojan orbits that dwarfs the simple adiabatic response due to a single migrating planet.

The effects of radial migration of all four giant planets on pre-existing Neptune Trojans have not received much attention. As far as we are aware, the only published study of the problem is

that of Gomes (1998). Gomes used both linear and exponential migration and found significant survival of Neptune Trojans in N-body simulations which had all four giant planets migrating. Gomes included 100 initial Trojan-type test particles and generally migrated the planets using the conventional Δa values given above. In linear migration models with a 10^6 year time scale Gomes found 82 particles survived as Neptune Trojans after migration. For a time scale of 10^7 years 53 Trojan particles survived. Using exponential migration, Gomes found that 30 Neptune Trojans survived for 2×10^7 years in a model with characteristic time scale $\tau = 1.5 \times 10^6$ years (τ is the e-folding time for migration) and that 49 survived 2×10^7 years with $\tau = 2.5 \times 10^6$ years, suggesting an increase in Trojan survivability with longer migration time scales. However, that trend was reversed in a model with $\tau = 10^7$ years, where Gomes found only 30 Neptune Trojans surviving for 5×10^7 years.

The relatively small number of initial test particles used by Gomes (1998) and the inconsistent results for different migration rates prevent a clear assessment of the general survivability of Neptune Trojans during primordial radial migration of the four giant planets. In addition, Gomes did not seek to identify the mechanism by which Neptune Trojans are destabilized during planetary migration. In the present paper we have re-evaluated the problem using more than an order of magnitude more particles. Our simulations use only exponential radial migration as this seems more realistic than linear migration (Fernández & Ip 1984, 1996; Hahn & Malhotra 1999). We find that there is a clear trend of decreasing Trojan survivability with increasing migration time scale. We also describe in detail the primary mechanism responsible for destabilization and loss of Neptune Trojans during migration. The remainder of this paper is organized as follows. In Section II we describe our initial conditions, the numerical model, and results from a series of simulations. In Section III we conclude by discussing some implications of our results in the context of our current understanding of planet migration and earlier work on Neptune Trojan stability.

II. METHOD AND RESULTS

IIa. Initial Conditions and Numerical Model

Unless otherwise noted, each of our simulations included the four giant planets Jupiter, Saturn, Uranus, and Neptune. The radial migration of these planets followed a smooth time variation of their semi-major axes, a. A time scale τ was used to characterize the migration, where $a(t) = a(0) + \Delta a[1 - \exp(-t/\tau)]$ and Δa is the desired amount of total migration at time $t = \infty$. Following Malhotra (1995), we adopt $\Delta a = -0.2$, 0.8, 3.0, and 7.0 AU, respectively for Jupiter, Saturn, Uranus, and Neptune. Table 1 lists the masses and initial configuration of these planets for our simulations. The masses of the terrestrial planets were added to the mass of the sun. Tab. 1

Orbital evolution was followed using the Wisdom-Holman (1991) symplectic integration technique with radial migration modifications included as non-gravitational forces (see Cordeiro *et al.* 1997). The mutual gravitational perturbations of the planets were included self-consistently even as their orbital spacing was expanding. The numerical simulation code is similar to that used in earlier work (Malhotra 1995). For all simulations we used a time step of 6 months, roughly 1/25 the orbital period of the innermost planet (Jupiter). This time step is sufficiently small to reliably integrate the orbits of the four giant planets and the test particles over the time scales we studied

(Wisdom & Holman 1992).

The initial conditions for the Neptune Trojans (modeled as massless test particles) were obtained as follows. We started with the population of Jupiter's current Trojan companions as of January 2002, a total of 1171 asteroids, having downloaded their orbital elements from the Minor Planet Center database (cfa-www.harvard.edu/iau/lists/JupiterTrojans.html). These asteroids are roughly evenly divided between Jupiter's leading L_4 (57%) and trailing L_5 (43%) Lagrange equilibrium regions. The orbital elements of these asteroids were then assigned to test particles at Neptune's initial orbit at 23 AU, with appropriate transformations of semi-major axes, arguments of pericenter, and longitudes of ascending node. Eccentricities and inclinations were not changed. This transformation was successful in placing most of the original population in 1:1 mean-motion resonance with Neptune. To verify this, during the first 25,000 years of each simulation we monitored the critical argument of each Neptune-Trojan pair, $\phi_{1:1}^{\rm NT} = \lambda - \lambda_{\rm Nep}$. All particles that maintained $0^\circ < |\phi_{1:1}^{\rm NT}| < 180^\circ$ for the first 25,000 years were considered members of the "initial" resonant population. This initial 25,000 years is about four times the libration period of $\phi_{1:1}^{\rm NT}$ for Neptune's initial orbit at 23 AU. Because of differences in the parameter τ, the number of particles in these initial populations at 25,000 years varied slightly in different simulations, but was always greater than 1000. During the remainder of each simulation $\phi_{1:1}^{\rm NT}$ for each particle was calculated every 100 time steps (50 years) and the extremal values of $\phi_{1:1}^{\rm NT}$ were updated every 10^4 years.

Our initial populations of Trojan particles (at $\mathsf{T}_{\rm o} = 25,000$ years) had a spread in semi-major axis $\Delta a \simeq 0.3$ AU, eccentricity $e \leq 0.2$, inclinations $i \leq 40^\circ$, and libration amplitudes $A \leq 150^\circ$. The range in (a, e, i) space for these initial populations covers roughly the same volume as the populations used by Nesvorný and Dones (2002) for their study of long term stability of Neptune Trojans subject to planetary perturbations in the present configuration of the solar system. They found that roughly 50% of the Neptune Trojan population survived after 4×10^9 years. A direct application of their stability results to our initial population is not possible because we used a different tighter planetary configuration. However, qualitatively their results suggest that our initial conditions more than adequately cover the most stable regions of the phase space for Neptune Trojans.

To increase run-time efficiency we removed particles from the simulations if their libration amplitude exceeded 180°. Thus, Neptune could not regain Trojans after they had been lost. A limited number of simulations were carried out that tracked all particles for the full duration of the simulation. In these simulations a small number of particles on large tadpole orbits around either the leading L_4 or trailing L_5 were found to be capable of transitioning to and from resonant horseshoe orbits as the planets migrated. However, recapture of lost Trojans by this process was a short-term effect. The counts of surviving Trojans in the primary runs typically differed only by one or two particles compared to the runs that followed all particles for the full duration of the simulation.

IIb. Migration Simulations

Figure 1 shows the evolution of the semi-major axes of the four giant planets as a function of time expressed in units of the characteristic migration time scale τ up to a time of 8τ. With this exponential migration model, radial migration of all planets is 99.33% complete after a time of 5τ. By this time orbital evolution of the planets (and of their Trojan companions) is dominated by gravitational perturbations from the planets in their near-final orbits rather than the effects of migration. Because the final configuration in each of our simulations cannot exactly match the current configuration of the solar system, we confine our study of Trojan survival to times less than or equal to 5τ. For stability analysis of Neptune Trojans beyond 5τ we defer to gigayear simulations that use the precise present orbital configuration of the solar system (Weissman & Levison 1997; Nesvorný & Dones 2002). These studies have shown that if a post-migration population of Neptune Trojans existed then some significant remnant (∼50%) should have survived on a 4 billion year time scale. Fig. 1

Figure 2 shows results from a relatively rapid migration simulation with $\tau = 10^6$ years. At the initial time $\mathsf{T}_o = 25,000$ years there were 1031 particles trapped in Neptune's leading L_4 and trailing L_5 regions. The top panel of Fig. 2 shows a histogram of the extremal values of $\phi_{1:1}^{\rm NT}$ for this initial population. The five lower panels of Fig. 2 show similar histograms of the Trojan population surviving after integer increments of the characteristic migration time scale τ. After a time of 5τ about 38% of the initial Trojan population remained in 1:1 resonance with Neptune. This result is reasonably consistent with that of Gomes (1998), who found a Neptune Trojan survival probability of 30-50% for $\tau = 1.5$ and 2.5×10^6 years. Fig. 2

Figure 3 shows results from a simulation where the migration rate was an order of magnitude slower than that of Fig. 2, with $\tau = 10^7$ years. The initial population at 25,000 years was nearly identical to the previous case, with 1025 test particles trapped in the leading and trailing Lagrange regions. However, after a time of 5τ most of the Trojans had been lost, with only 1.5% of the initial population surviving. The simulations shown in Figs. 2 and 3 represent examples of our key result: survivability of Neptune Trojans depends on the characteristic migration time scale. Although the simulation with $\tau = 10^7$ years ran for 10 times longer than that with $\tau = 10^6$ years, the greater losses in Fig. 3 cannot be explained simply by the longer duration of the simulation. In neither case were the losses the result of a gradual random diffusive process. Fig. 3

Because of the inherent chaotic nature of N-body simulations, identical initial conditions modeled on different computers (different processors and/or compilers) produced results that were generally in agreement but differed in some details. For example, some Trojans lost after 5τ in a $\tau = 10^7$ year simulation on a Sun Sparc Ultra 5 were survivors when the simulation was run on an Intel Xeon CPU, and vice versa. We ran simulations for each value of τ on four different types of processors – the Sparc, two Xeons (1.7 and 2.4 GHz), and a Digital Alpha EV6. Figure 4 shows a composite histogram of the survivability of Neptune Trojans from runs on these four types of processors for simulations with $\tau = 10^6, 2.5 \times 10^6, 5 \times 10^6$, and 10^7 years. These four runs for each value of τ effectively quadruple the number of initial test particles in each case, resulting in over 4000 initial Trojan test particles for each value of τ. Figure 4 displays an obvious trend: Neptune loses Trojans during migration and it loses more Trojans for longer migration time scales. Com- Fig. 4

paring the survival statistics in Fig. 4 at equal durations in time (e.g., at 5×10^6 years for different values of τ) reveals that these losses cannot be explained by a constant diffusion with time.

In all simulations shown in Fig. 4 Neptune is migrating from just exterior to the 3:5 mean-motion resonance with Uranus to approximately its present orbit just interior to the 1:2 mean-motion resonance with Uranus (see Fig. 1). Between the 3:5 and 1:2, Neptune and its Trojans cross numerous other higher order uranian resonances, such as the 4:7 and 5:9. All of these resonances play a role in destabilizing Neptune Trojans during migration. Simple confirmation of this was found by repeating some simulations without Uranus (see Fig. 5). In these simulations nearly all initial Neptune Trojan particles survived to a time of 5τ. Fig. 5

The importance of Uranus in this problem should not be entirely unexpected. In an ideal case Uranus is the planet that comes the closest to, and strays the farthest from, Neptune's Trojans. For a Trojan initially trapped exactly at Neptune's L_4 or L_5 point (zero libration amplitude), Uranus passes within 7 AU at conjunction and is as distant as 39 AU at opposition. Neptune, on the other hand, remains at a distance of 23 AU. Accounting for the difference in planetary mass, the gravitational force from Uranus acting on the particle varies, from about nine times stronger than the force from Neptune at conjunction to about one third weaker at opposition. These uranian perturbations will repeat with the synodic period of Uranus and Neptune. For a Trojan particle with non-zero libration amplitude, its position will vary somewhat at each conjunction with Uranus. Thus, the uranian perturbations, while roughly of the same magnitude, will at times accelerate and others decelerate the particle's motion with respect to Neptune. The net effect over many libration periods amounts to destructive interference which does not destabilize the Trojan particle's resonant configuration with Neptune. However, if the Uranus-Neptune-Trojan orbital orientation becomes periodic in time (a three-body resonance) then the uranian perturbations could buildup constructively, driving the Trojan particle to larger or smaller libration amplitude.

Note that for the initial conditions in Tab. 1 the gravitational forces acting on Neptune's Trojans from Saturn and Jupiter are always larger than the force from Neptune. Saturnian perturbations range from about 13 to 3 times those from Neptune, at conjunction and opposition with the Trojan particle, respectively. Jovian perturbations are stronger still, 30 times neptunian at conjunction and 12 times at opposition. The high retention of Trojans in simulations that did not include Uranus (Fig. 5) demonstrate that the direct saturnian and jovian perturbations do not dominate the stability of Neptune Trojans during planetary migration. Jupiter and Saturn have short synodic periods with respect to Neptune (about 14 and 34 years). Considering the $\sim 10^4$ year libration period of Neptune's Trojans, the high frequency low amplitude perturbations from Saturn and Jupiter can be considered in an orbit-averaged sense, as if the mass of these two distant planets were distributed in a ring about their orbits. Results shown in Fig. 5 and the simple schematic described above do not preclude destabilizing roles for Jupiter and Saturn acting indirectly through perturbations on Uranus (Michtchenko *et al.* 2001).

Close scrutiny of the orbital evolution of some of the Trojans lost in our simulations strengthens the case against Uranus acting alone. Figure 6 provides an example of the evolution of Trojan libration amplitudes in a simulation with $\tau = 5 \times 10^6$ years. In this simulation about 95% of the initial population of Neptune Trojans was lost by a time of 5τ. Nearly all Trojans that were lost Fig. 6

between a time of τ and 5τ evolved out of resonance during a discrete number of prolonged episodes. The top panel of Fig. 6 shows these events, with numerous particles cascading out of resonance together. Figure 6 also shows selected examples of some lost Trojans (middle panel) and others that survive these events (bottom panel). In general, the cascading episodes that occur earlier affect only those Trojans with relatively large libration amplitudes, with more tightly bound particles affected by each subsequent episode. This suggests that the cause of these events is gaining strength with time. Note also that during any given single cascading episode smaller libration amplitude (higher lib. freq.) particles are affected first and larger libration amplitude (lower lib. freq.) particles are picked up as the episode progresses. Also, the time between episodes, from the beginning of one to the beginning of the next, increases systematically by about a factor of two. These time-dependent features suggest that the cause has a characteristic frequency that is slowing appreciably during the course of each episode and from one episode to the next. Finally, those Trojans that survive the episodes (bottom panel, Fig. 6) experience sharp changes in libration amplitude at times coincident with other particles of similar libration amplitude being swept up in an event. Figure 6 is an example from a simulation with $\tau = 5 \times 10^6$ years but the general characteristics of the cascading episodes were similar for all values of τ. The primary difference was that the number of particles lost during each event increased as τ increased.

Many of these features are similar to the effects of sweeping secondary resonances studied in the tidal evolution of the uranian satellite system (Tittermore & Wisdom 1990; Malhotra & Dermott 1990; Malhotra 1998a). In particular, the anomalously large orbital inclination of Miranda is naturally explained as a consequence of secondary resonance sweeping due to tidal evolution within a 3:1 inclination-type mean-motion resonance with Umbriel. This resonance increased Miranda's inclination from an initially small value, but the resonance was temporary. As Miranda's inclination approached its current value, the satellites were captured in a secondary resonance which amplified their primary resonance libration amplitude; this eventually caused the satellites to escape from the 3:1 mean-motion resonance, leaving Miranda with an inclination that is preserved to the present. The secondary resonance implicated in this case was due to a 1:3 commensurability between the libration frequency of the mean-motion resonance angle and the secular frequency of precession of the relative lines of nodes of the two satellites. The exact secondary resonance can be identified because each one is associated with a specific value of the final inclination of Miranda.

The essential elements of the Uranian satellite dynamics relevant to the present work are that (i) secondary resonances appear at the center of the primary resonance, initially at small libration amplitude, and sweep across the entire libration region of the primary resonance; (ii) capture into a secondary resonance is a probabilistic phenomenon, with low-integer secondary resonances having generally higher probabilities of capture; (iii) capture in a secondary resonance causes an amplification of the libration amplitude until the system escapes the mean-motion resonance; (iv) particles not captured experience a small perturbation, mainly in their libration amplitude; they may later be captured by another secondary resonance sweeping by. This analogy suggests that the cascading episodes of Neptune's Trojans found in our models (Fig. 6) are caused by one or more secondary resonances sweeping across the phase space occupied by the Trojan particles. Some Trojan particles can be trapped in these secondary resonances and forced out of Neptune's Lagrange regions. Others only experience a momentary perturbation as a secondary resonance

crosses their location in phase space.

During the cascading episodes shown in Fig. 6 the strongest resonance in the vicinity of Neptune and its Trojan particles is the 1:2 mean-motion with Uranus. While Uranus and Neptune are not locked in 1:2 resonance with each other, they are close. One critical argument for the Uranus-Neptune near-resonance is $\phi^{\rm UN}_{1:2} = 2\lambda_{\rm Nep} - \lambda_{\rm Ura} - \tilde{\omega}_{\rm Ura}$, where $\tilde{\omega}_{\rm Ura}$ is the longitude of pericenter for Uranus. During migration $\phi^{\rm UN}_{1:2}$ circulates through all angles 0 to 360° while the Neptune-Trojan critical argument, $\phi^{\rm NT}_{1:1}$, librates about ±60°. The libration frequency of $\phi^{\rm NT}_{1:1}$, given as $f^{\rm NT}_{1:1}$, is $\sim 10^{-4}$ yr^{-1} and decreases only slightly as Neptune migrates outward ($\propto a_{\rm Nep}^{-3/2}$). The circulation frequency of $\phi^{\rm UN}_{1:2}$, given as $f^{\rm UN}_{1:2}$, is initially more rapid than $f^{\rm NT}_{1:1}$ but decreases dramatically as the migrating Uranus and Neptune converge upon 1:2 resonance. As $f^{\rm UN}_{1:2}$ converges toward $f^{\rm NT}_{1:1}$ Trojan particles can become trapped in secondary resonances that occur when $f^{\rm UN}_{1:2}$ becomes commensurate with harmonics of $f^{\rm NT}_{1:1}$, where $f^{\rm UN}_{1:2} \approx (j/k) f^{\rm NT}_{1:1}$, j and k are integers, and $j \geq k$.

Figure 7 shows an example from a $\tau = 10^7$ year simulation where a Trojan particle was lost while trapped in a 1:4 commensurability between $f^{\rm UN}_{1:2}$ and $f^{\rm NT}_{1:1}$. A fast Fourier filter (FFT) was used to obtain power spectra of $\phi^{\rm NT}_{1:1}$ (middle panel) and $\phi^{\rm UN}_{1:2}$ (bottom panel). Spectra were taken every $0.1\,\tau$ (10^6 years) from 1.4 to 2.8τ. Each FFT used 4096 points sampled every 100 years, giving an FFT interval of about 0.041τ. In the first interval, starting at 1.4τ, $f^{\rm UN}_{1:2}$ is higher than the 6th harmonic of $f^{\rm NT}_{1:1}$. As Uranus and Neptune converge upon the 1:2 resonance $f^{\rm UN}_{1:2}$ slows and passes the $6^{\rm th}$ harmonic of $f^{\rm NT}_{1:1}$ at about 1.55τ. The libration amplitude of the Trojan particle experiences a perturbation at this time. Passage of $f^{\rm UN}_{1:2}$ by the $5^{\rm th}$ harmonic of $f^{\rm NT}_{1:1}$ at 1.85τ results in a more significant change in libration amplitude. At about 2.23τ the $4^{\rm th}$ harmonic is reached, where $f^{\rm UN}_{1:2} \approx 4 f^{\rm NT}_{1:1}$. After 2.23τ, as Uranus and Neptune migrate closer to 1:2 resonance the particle is captured in this 1:4 secondary resonance between $f^{\rm UN}_{1:2}$ and $f^{\rm NT}_{1:1}$; as a consequence it is gradually forced to larger libration amplitude. Increasing libration amplitude results in a slower libration frequency. Thus, the $4^{\rm th}$ harmonic of the slowing $f^{\rm NT}_{1:1}$ keeps pace with the slowing $f^{\rm UN}_{1:2}$. The particle is trapped and the 1:4 secondary resonance is maintained. Trapped particles forced to libration amplitudes of 110 to 130° were quickly lost from Neptune's Lagrange regions. Fig. 7

Initially, $f^{\rm UN}_{1:2}$ is more than a factor of 10 faster than $f^{\rm NT}_{1:1}$. After a time of 5τ Uranus and Neptune have reached nearly their final orbits and $f^{\rm UN}_{1:2}$ is less than twice as fast as $f^{\rm NT}_{1:1}$ for a typical unaffected Trojan particle. As $f^{\rm UN}_{1:2}$ slows it passes numerous higher harmonics of $f^{\rm NT}_{1:1}$. The occurrences of commensurabilities between $f^{\rm UN}_{1:2}$ and harmonics of $f^{\rm NT}_{1:1}$ correspond precisely to the cascading episodes shown in Fig. 6. In the middle panel of Fig. 6 the last particle lost (near 4.8τ) was initially tightly bound to Neptune's L_4 or L_5 with a libration amplitude below 10°. This particle became trapped in a 1:2 secondary resonance, $f^{\rm UN}_{1:2} \approx 2 f^{\rm NT}_{1:1}$, and was lost in about 5×10^6 years. The first particle lost in the examples of Fig. 6 (near 1.5τ) was likely trapped in the 1:11 secondary resonance. The 1:9 and 1:10 commensurabilities are not represented in the examples shown in Fig. 6.

In all simulations significant loss of Neptune Trojans occurred in the first multiple of τ, before the first bars on the histogram of Fig. 4. An example of Trojan evolution during this early period is shown in Fig. 8 for a simulation with $\tau = 10^7$ years. The format is similar to Fig. 6, with a cross-section of particles shown at the top, examples of lost Trojans in the middle panel, and two Figs. 8,9

typical survivors at the bottom. As in Fig. 6, loss of Trojans is confined to a few discrete episodes, primarily from 0.12–0.24τ and 0.32–0.44τ. Because these losses occur so early in the migration process the 3:5 and 4:7 Uranus-Neptune mean-motion resonances are likely culprits. Figure 9 shows a detailed analysis of one Trojan particle lost at 0.44τ. Spectra of $\phi_{1:1}^{\rm NT}$ (middle panel) are shown in comparison with spectra (bottom panel) of a critical argument of the Uranus-Neptune 4:7 mean-motion near-resonance, $\phi_{4:7}^{\rm UN} = 7\lambda_{\rm Nep} - 4\lambda_{\rm Ura} - 3\tilde{\omega}_{\rm Ura}$. Initially, as Uranus and Neptune approach 4:7 resonance the circulation frequency of the critical argument, $f_{4:7}^{\rm UN}$, slows and converges upon $f_{1:1}^{\rm NT}$. Abrupt changes in the Trojan libration amplitude record passage of $f_{4:7}^{\rm UN}$ by the 3$^{\rm rd}$, 2$^{\rm nd}$, and 1$^{\rm st}$ harmonics of $f_{1:1}^{\rm NT}$. This particular Trojan survives these events but Fig. 8 illustrates that many particles are lost in events leading up to the 1:1 commensurability between $f_{4:7}^{\rm UN}$ and $f_{1:1}^{\rm NT}$. At about 0.27τ all of the power in the spectrum of $\phi_{4:7}^{\rm UN}$ falls near zero frequency. This indicates that circulation of $\phi_{4:7}^{\rm UN}$ has ceased, with Uranus and Neptune crossing their 4:7 resonance. As the planets withdraw from the 4:7 resonance circulation of $\phi_{4:7}^{\rm UN}$ resumes and speeds up, with $f_{4:7}^{\rm UN}$ now diverging from $f_{1:1}^{\rm NT}$. Divergent passages of $f_{4:7}^{\rm UN}$ by harmonics of $f_{1:1}^{\rm NT}$ result in abrupt changes to the particle's libration amplitude. The particle is finally lost following passage of $f_{4:7}^{\rm UN}$ by the 8$^{\rm th}$ harmonic of $f_{1:1}^{\rm NT}$.

The effects of secondary resonances demonstrated by Figs. 7 and 9 can be used to associate gross features seen in Figs. 6 and 8 with their respective causes. In Fig. 8 the initial loss of Trojans between 0 and 0.06τ corresponds to withdrawal of Uranus and Neptune from the location of their 3:5 mean-motion resonance. Between 0.12 and 0.24τ the planets are approaching their 4:7 resonance. The lull from 0.24 to 0.3τ corresponds to a calm period when the planets actually cross the location of their 4:7 resonance. Withdrawal from the 4:7 leads to more lost Trojan particles between 0.3 and 0.44τ. Structure from 0.44 to 0.58τ is from approach to the 5:9, with withdrawal from 5:9 between 0.6 and 0.8τ. We can also see structure associated with approach to and withdrawal from the 6:11 resonance, between 0.8 and 1.1τ (more evident in Fig. 6). The two survivors shown as examples in the bottom panel of Fig. 8 show sudden changes in libration amplitude probably caused by secondary resonances associated with the 6:11 resonance.

Loss of Neptune Trojans during secondary resonances with Uranus and Neptune occurred for all values of τ. However, the fraction lost during passages of each secondary resonance increased as τ increased. Figure 4 essentially gives the results for loss during approach to the Uranus-Neptune 1:2 mean-motion resonance. With $\tau = 10^6$ years about 50% of the Trojan particles still present are lost through secondary resonances associated with the 1:2. With $\tau = 10^7$ years about 85% of existing Trojans are lost during these same events. For times less than τ Fig. 4 provides bulk survival statistics for events associated with higher order Uranus-Neptune resonances such as the 3:5, 4:7, and 5:9. These include withdrawal from the 3:5 as well as approach and withdrawal from both the 4:7 and 5:9. With $\tau = 10^6$ years about 20% of Trojan particles are lost through secondary resonances associated with all these events. In contrast, with $\tau = 10^7$ years nearly 65% of Trojan particles are lost during the same events.

Most of the Trojans lost in our simulations were destabilized by perturbations from Uranus. The primary episodes of loss can be directly linked to the secondary resonances described above. The nearest saturnian and jovian mean-motion resonances to Neptune are the saturnian 1:6 and jovian 1:13 and 1:14. Direct perturbations of Jupiter and Saturn on Neptune Trojans appear to

play a very minor role, as indicated by results from the simulation run without Uranus. Indirect perturbations of Jupiter and Saturn, acting through Uranus, may have a greater influence. One important mean-motion resonance in the region of Uranus is the jovian 1:7. The pair cross their 1:7 mean-motion resonance between 3.25τ and 3.5τ (see Fig. 1). Figure 6 shows that some Trojan particles trapped in the 1:3 secondary resonance ($f_{1:2}^{\rm UN} \approx 3 f_{1:1}^{\rm NT}$) are lost in this time interval. Spectral analysis of some of these trapped particles indicates that they can escape the secondary resonance during passage of the Jupiter-Uranus 1:7 mean-motion resonance. It is possible then that some of the Trojan particles forced to high libration amplitudes while trapped in the 1:3 secondary resonance could ultimately have been lost as a result of the Jupiter-Uranus 1:7 mean-motion resonance.

III. DISCUSSION

The post-formation orbital evolution of the giant planets in our solar system is constrained by observed characteristics of small body populations. Studies of the interaction of the giant planets with these populations have led to a detailed understanding of the early dynamical evolution of the outer solar system. Discovery of the first Trojan companion of Neptune, 2001 QR 322, reveals yet another class of minor solar system body. As more of these objects are discovered, statistical comparisons of their orbits with results from numerical modeling such as ours will provide further constraints on the early history of the solar system. With only a single known Neptune Trojan, such a comparison may not carry much weight but is still interesting. Figure 10 shows the initial and final distributions of eccentricity, inclination, and libration amplitude for surviving Trojans from the $\tau = 10^7$ year simulation. The initial and final distributions of inclination and libration amplitude show no strong differences. The eccentricity distributions are markedly different though. Figure 11 shows the mean eccentricity of surviving Trojan particles as a function of time for all values of τ. The initial eccentricities of the particles (at $\mathsf{T}_{\rm o} = 25,000$ years) were about equal to those of Jupiter's real Trojan asteroids, with a mean of 0.075 and standard deviation of about ± 0.03. The secondary resonances primarily removed higher eccentricity particles and longer migration time scales led to erosion of lower eccentricity particles. With $\tau = 10^7$ years the surviving population at 5τ has a mean eccentricity of 0.04 ± 0.02. Figs. 10,11

The (a, e, i) space occupied by the surviving Neptune Trojans in our $\tau = 10^7$ years simulation overlaps remarkably well with the large stable region found by Nesvorný and Dones (2002). In their study, using the present configuration of the planets as starting conditions, nearly all Trojan particles within ± 0.1 AU of the libration center and with $e \leq 0.07$, $i \leq 25°$, $A \leq 60 - 70°$ survived for 4×10^9 years. The agreement is probably not coincidental considering the importance we found for the 1:2 mean-motion near-resonance between Uranus and Neptune. Nesvorný and Dones found that this same near-resonance shapes the stability of Neptune's Trojan regions in the present planetary configuration. The similarity between our final conditions for $\tau = 10^7$ years and the initial conditions of Nesvorný and Dones suggests that 30 to 50% of Neptune's post-migration Trojan population could survive for the age of the solar system. This indicates that Neptune's current Trojan population may be just 1-2% of its primordial size.

Depending on initial conditions it may be possible to either mitigate or enhance Trojan losses during planetary migration. From the characteristics of Pluto's orbit, Malhotra (1995) shows that 5 AU should be considered a minimum migration distance for Neptune. This smaller distance could

allow Neptune Trojans to avoid destabilizing secondary resonances associated with withdrawal from the 3:5 with Uranus and some of those associated with approach to the 4:7. On the other hand, Gomes (1997) suggests that Neptune may have migrated as much as 9–10 AU rather than the nominal value of 7 AU assumed in our simulations. The extra 2 AU would put Neptune initially interior to the location of the 3:5 mean-motion resonance with Uranus. Neptune Trojans would then be subject to additional losses through secondary resonances associated with approach to the 3:5. Convergence of Uranus and Neptune toward 1:2 mean-motion resonance seems unavoidable based on our current understanding of planetary migration. Therefore, regardless of the extent of Neptune's migration (be it 5, 7, or 9 AU), it is the migration rate on final approach to its present orbit that determined the fate of most of its Trojans.

Previous work (Malhotra 1998b) suggests that planetary migration with $\tau = 10^7$ years is favored to allow Kuiper belt objects trapped in 2:3 mean-motion resonance with Neptune to evolve to the high orbital inclinations observed for some of the plutinos. If Neptune had an abundant primordial population of Trojan companions then migration with $\tau \geq 10^7$ years would have dramatically depleted that population. The loss rate would not have been a smooth function of time. Instead, the losses would have been episodic, with an especially dramatic loss between 4 and 5τ as Uranus and Neptune closed upon their present near-resonant configuration. Our simulations show that this final loss episode involved a nearly 75% reduction in Neptune's Trojan population (see Fig. 4). These liberated bodies, heretofore dynamically sequestered by Neptune, would be injected into the largely eroded planetesimal disk. We speculate that if their numbers were sufficiently high they could have temporarily enhanced the impact rate throughout the solar system. Traces of this event, while probably not preserved in Triton's relatively fresh surface, may be preserved in the impact records on other more ancient surfaces.

IV. ACKNOWLEDGMENTS

We thank Bill Hartmann and Stu Weidenschilling for valuable comments on an early draft of this paper. This material is based upon work supported by the National Aeronautics and Space Administration under Grant Nos. NAG5-10343 and NAG5-11661 issued through the Office of Space Science and by the Research Foundation of São Paulo State (FAPESP) under Grant No. 01/13447-6.

V. REFERENCES

Chen, J., D. Jewitt, C. Trujillo, and J. Luu 1997. Mauna Kea Trojan survey and statistical studies of L_4 Trojans. *Bull. Amer. Astron. Soc.* **29**, DPS abstract #25.08.

Chiang, E.I., and A.B. Jordan 2002. On the plutinos and twotinos of the Kuiper belt. *Astron. J.* **124**, 3430–3444.

Chiang, E.I. 2003. 2001 QR 322. *IAU Circulars* 8044.

Cordeiro, R.R., R.S. Gomes, and R.V. Martins 1997. A mapping for nonconservative systems. *Celes. Mech. Dynamic. Astron.* **65**, 407–419.

de la Barre, C.M., W.M. Kaula, and F. Varadi 1996. A study of orbits near Saturn's triangular Lagrangian points. *Icarus* **121**, 88–113.

Fernandez, J.A., and W.H. Ip 1984. Some dynamical aspects of the accretion of Uranus and Neptune: The exchange of orbital angular momentum with planetesimals. *Icarus* **58**, 109–120.

Fernandez, J.A., and W.H. Ip 1996. Orbital expansion and resonant trapping during the late accretion stages of the outer planets. *Plan. Spa. Sci.* **44**, 431–439.

Fleming, H.J., and D.P. Hamilton 2000. On the origin of the Trojan asteroids: Effects of Jupiter's mass accretion and radial migration. *Icarus* **148**, 479–493.

Friedland, L. 2001. Migration timescale thresholds for resonant capture in the plutino problem. *Astrophys. J. Lett.* **547**, 75–79.

Gomes, R.S., 1997. Orbital evolution in resonance lock I. The restricted 3-body problem. *Astron. J.* **114**, 2166–2176.

Gomes, R.S., 1998. Dynamical effects of planetary migration on primordial Trojan-type asteroids. *Astron. J.* **116**, 2590–2597.

Gomes, R.S., 2000. Planetary migration and plutino orbital inclinations. *Astron. J.* **120**, 2695–2707.

Gomes, R.S. 2003. The origin of the Kuiper belt high-inclination population. *Icarus* **161**, 404–418.

Hahn, J.M., and R. Malhotra 1999. Orbital evolution of planets embedded in a planetesimal disk. *Astron. J.* **117**, 3041–3053.

Holman, M.J., and J. Wisdom 1993. Dynamical stability in the outer solar system and the delivery of short period comets. *Astron. J.* **105**, 1987–1999.

Liou, J.C., and R. Malhotra 1997. Depletion of the outer asteroid belt. *Science* **275**, 375–377.

Malhotra, R., 1993. The origin of Pluto's peculiar orbit. *Nature* **365**, 819–821.

Malhotra, R., 1995. The origin of Pluto's orbit: Implications for the solar system beyond Neptune. *Astron. J.* **110**, 420–429.

Malhotra, R., 1998a. Orbital resonances and chaos in the solar system, In *Solar System Formation and Evolution*, (D. Lazzaro, R. Vieira Martins, S. Ferraz-Mello, J. Fernández, and C. Beaugé, Eds.), ASP Conference Series **149**, pp. 37–63.

Malhotra, R., 1998b. Pluto's inclination excitation by resonance sweeping. *Lunar Planet. Sci. Conf.* **29**, abstract # 1476 on CD-ROM.

Malhotra, R., and S.F. Dermott 1990. The role of secondary resonances in the orbital history of Miranda. *Icarus* **85**, 444–480.

Malhotra, R., M. Duncan, and H. Levison 2000. Dynamics of the Kuiper belt. In *Protostars and Planets IV*, (V. Mannings, A.P. Boss, and S.S. Russell, Eds.) pp. 1231–1254. Univ. Arizona Press, Tucson.

Marsden, B.G. 2003. 2001 QR 322. *Minor Planet Ele. Circulars* 2003-A55.

Michtchenko, T.A., C. Beaugé, and F. Roig 2001. Planetary migration and the effects of mean motion resonances on Jupiter's Trojan asteroids. *Astron. J.* **122**, 3485–3491.

Nesvorný, D., and L. Dones 2002. How long-lived are the hypothetical Trojan populations of Saturn, Uranus, and Neptune? *Icarus* **160**, 271–288.

Tittemore, W.C., and J. Wisdom 1990. Tidal evolution of the uranian satellites III. Evolution through the Miranda-Umbriel 3:1, Miranda-Ariel 5:3, and Ariel-Umbriel 2:1 mean-motion commensurabilities. *Icarus* **85**, 394–443.

Weissman, P.R., and H.F. Levison 1997. The population of the trans-neptunian region: The Pluto-Charon environment. In *Pluto and Charon*, (S.A. Stern and D.J. Tholen, Eds.), pp. 559–604. Univ. Arizona Press, Tucson.

Wisdom, J., and M. Holman 1991. Symplectic maps for the N-body problem. *Astron. J.* **102**, 1528–1538.

Wisdom, J., and M. Holman 1992. Symplectic maps for the N-body problem: Stability analysis. *Astron. J.* **104**, 2022–2029.

Table 1
Initial Heliocentric Planetary Configuration[b]

Planet	Mass Semi-Major Axis Long. Ascend. Node	Eccentricity Arg. Pericenter	Inclination Mean Anomoly
Jupiter	9.54791810627724E−04		
	5.40430411233366E+00	4.90137254366321E−02	6.88824194620820E−03
	5.45582894296211E+00	1.08695015636752E+00	5.07600450707522E−01
Saturn	2.85585440033128E−04		
	8.78367171921144E+00	5.62633466451345E−02	1.49881886264974E−02
	2.18380557155612E+00	5.67051860572230E+00	5.55873741721312E+00
Uranus	4.37275778048887E−05		
	1.63160636907320E+01	4.47359382069131E−02	1.91275920013027E−02
	5.41937420992345E+00	3.71536831241412E+00	4.48013898742567E+00
Neptune	5.17762233001967E−05		
	2.29867881794121E+01	1.18546237182779E−02	1.26187650361650E−02
	3.49327271961024E+00	3.51610962057474E+00	2.33495547884702E+00

[b]Solar masses, AUs, radians referred to invariable plane and mean equinox, Epoch 243000.5

Figure Captions

Figure 1: Four panels showing examples of the evolution with time of the semi-major axes of the four giant planets in a migration simulation. The planets were subject to mutual gravitational perturbations and a drag force which caused their orbits to migrate—Jupiter inward; Saturn, Uranus, and Neptune outward. Table 1 gives the initial orbital parameters for the planets. Time is expressed in units of τ, the characteristic migration time scale. After a time of 5τ migration is 99.33% complete and subsequent orbital evolution is dominated by mutual planetary gravitational perturbations rather than the migration force. Dashed lines indicate the ideal locations (for zero eccentricity) of the 3:5 and 1:2 mean-motion resonances with Uranus and the 1:7 mean-motion resonance with Jupiter.

Figure 2: Survival of Neptune Trojans in a simulation with the four giant planets migrating with a characteristic time scale of $\tau = 10^6$ years. The six panels show minimum and maximum limits on libration of the critical argument, $\phi_{1:1}^{\rm NT} = \lambda - \lambda_{\rm Nep}$. The dashed lines at $\pm 60^\circ$ indicate the ideal locations of the leading L_4 and trailing L_5 Lagrange equilibrium points (for zero eccentricity). Each histogram gives the number of surviving Trojans in each bin as a fraction of the total population across all bins at the initial time $\mathsf{T}_{\rm o} = 25,000$ years. The top panel shows the initial distribution at time $\mathsf{T}_{\rm o}$. Each of the subsequent lower panels lists the output time in units of τ and the number of particles trapped in the L_4 and L_5 regions.

Figure 3: Similar to Fig. 2 but from a simulation with characteristic time scale 10 times slower, $\tau = 10^7$ years. All other initial conditions were identical to the simulations shown in Fig. 2. In this slow migration simulation nearly 99% of Neptune's initial Trojan companions are lost after 5τ.

Figure 4: Histogram of the surviving fraction of Neptune Trojans as a function of time for four different characteristic migration time scales, τ, ranging from 10^6 to 10^7 years. In each case, time is expressed as integer multiples of τ up to 5τ. Solid and open bars indicate surviving fractions of Trojans in Neptune's leading L_4 and trailing L_5 regions, respectively. For each value of τ, simulations with identical initial conditions were run on four different types of processors, two Intel Xeons (1.7 and 2.4 GHz), a Digital Alpha EV6, and a Sun Sparc Ultra 5. The results shown in the histogram are a composite from all four simulations.

Figure 5: Similar to Fig. 2 ($\tau = 10^7$) but from a simulation that included Jupiter, Saturn, and Neptune, but not Uranus. Removing Uranus resulted in nearly full retention of Neptune Trojans up to a time of 5τ.

Figure 6: The libration amplitude of Neptune Trojans as a function of time expressed in units of τ for a simulation with $\tau = 5 \times 10^6$ years. Evolution of the general population is shown in the top panel. To avoid saturation only every fifth particle is plotted and libration amplitudes greater than 180° are not connected. After a time of τ, loss of Trojans is generally marked by cascading of particles out of resonance during a discrete number of prolonged events.

Examples of Trojans lost during these episodes are shown in the middle panel. Trojans not lost by this process are still perturbed and can have their libration amplitudes decreased, as seen in the descending step-like appearance of the libration amplitudes of the survivors shown in the bottom panel.

Figure 7: Evolution of the libration amplitude for one of the lost Trojans from a $\tau = 10^7$ year simulation is shown here at high resolution (top panel). A fast Fourier transform (FFT) was used to obtain power spectra of critical arguments for both the Neptune-Trojan 1:1 resonance ($\phi_{1:1}^{\rm NT} = \lambda - \lambda_{\rm Nep}$, middle panel) and the Uranus-Neptune 1:2 near-resonance ($\phi_{1:2}^{\rm UN} = 2\lambda_{\rm Nep} - \lambda_{\rm Ura} - \tilde{\omega}_{\rm Ura}$, bottom panel). Each FFT used 4096 points sampled every 100 years (see FFT interval bar), resulting in a Nyquist critical frequency (5 kyr^{-1}) well removed from the range shown here. The start times of the FFTs are indicated to the right of the spectra. Spectra of $\phi_{1:1}^{\rm NT}$ (middle panel) are shown in units of log power in order to simultaneously resolve the fundamental frequency ($f_{1:1}^{\rm NT}$) and its higher harmonics. The initial positions of the first six harmonics of $f_{1:1}^{\rm NT}$ are indicated by the dashed lines. As $f_{1:2}^{\rm UN}$ converges toward $f_{1:1}^{\rm NT}$ it overtakes the 6$^{\rm th}$ and then the 5$^{\rm th}$ harmonics of $f_{1:1}^{\rm NT}$. The Trojan particle experiences sudden changes in libration amplitude during these passages (indicated in top panel). At about $2.23\,\tau$ (see spectra taken at $2.2\,\tau$) the 4$^{\rm th}$ harmonic of $f_{1:1}^{\rm NT}$ becomes locked to $f_{1:2}^{\rm UN}$.

Figure 8: Similar to Fig. 6 except shown at higher temporal resolution for the period from time 0 to τ.

Figure 9: Similar to Fig. 7. The libration amplitude of one Trojan particle from Fig. 8 is shown at higher resolution (top panel). Power spectra of $\phi_{1:1}^{\rm NT}$ (middle panel, in log power) are compared with spectra of a critical argument for the 4:7 mean-motion resonance with Uranus ($\phi_{4:7}^{\rm UN} = 7\lambda_{\rm Nep} - 4\lambda_{\rm Ura} - 3\tilde{\omega}_{\rm Ura}$). Spectra were taken every 0.02τ (2×10^5 years) from 0.21 to 0.43τ (labeled to right of spectra). Each FFT used 1024 points sampled every 100 years, giving an FFT interval (indicated in top panel) of about 0.01τ. Note that dashed lines only indicate initial locations of the first six harmonics of $f_{1:1}^{\rm NT}$. By the later spectra, $f_{1:1}^{\rm NT}$ has slowed sufficiently to move the 8$^{\rm th}$ harmonic into the frame.

Figure 10: Histograms showing the distributions of eccentricity, inclination, and libration amplitude from the $\tau = 10^7$ year simulations. The dashed line indicates the initial distribution at $\mathsf{T}_{\rm o} = 25,000$ years and the solid line is the final distribution after 5τ. N indicates the number of Trojan particles remaining after $\mathsf{T}_{\rm o}$ and 5τ. The orbital eccentricity of 2001 QR 322 is also indicated.

Figure 11: Distribution of orbital eccentricity of the surviving Neptune Trojans as a function of time for four different characteristic migration time scales, τ, ranging from 10^6 to 10^7 years. Points are the mean and error bars are one standard deviation. The orbital eccentricity of 2001 QR 322 is shown by the dashed line.

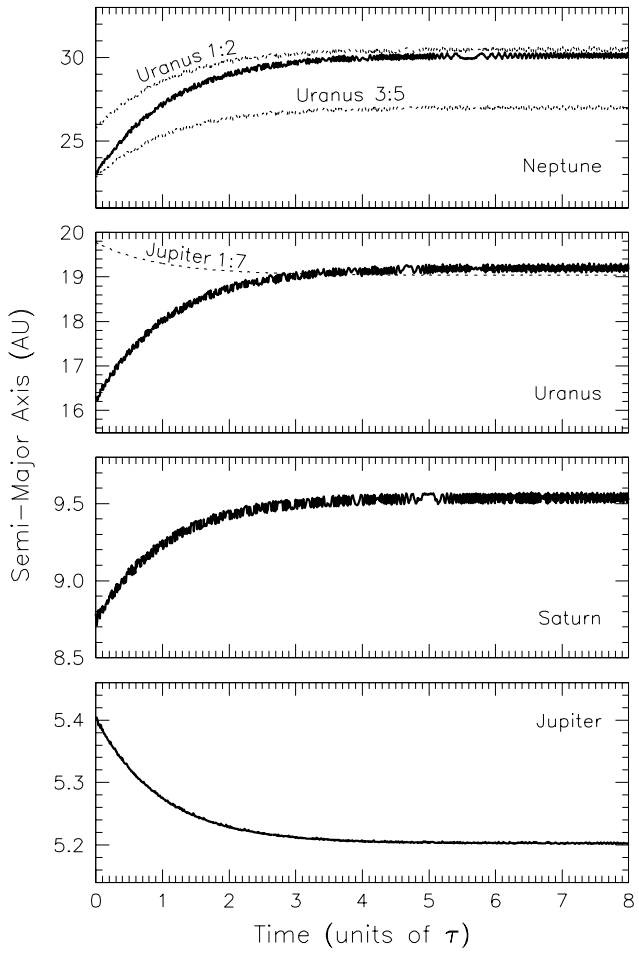

Figure 1: Four panels showing examples of the evolution with time of the semi-major axes of the four giant planets in a migration simulation. The planets were subject to mutual gravitational perturbations and a drag force which caused their orbits to migrate—Jupiter inward; Saturn, Uranus, and Neptune outward. Table 1 gives the initial orbital parameters for the planets. Time is expressed in units of τ, the characteristic migration time scale. After a time of 5τ migration is 99.33% complete and subsequent orbital evolution is dominated by mutual planetary gravitational perturbations rather than the migration force. Dashed lines indicate the ideal locations (for zero eccentricity) of the 3:5 and 1:2 mean-motion resonances with Uranus and the 1:7 mean-motion resonance with Jupiter.

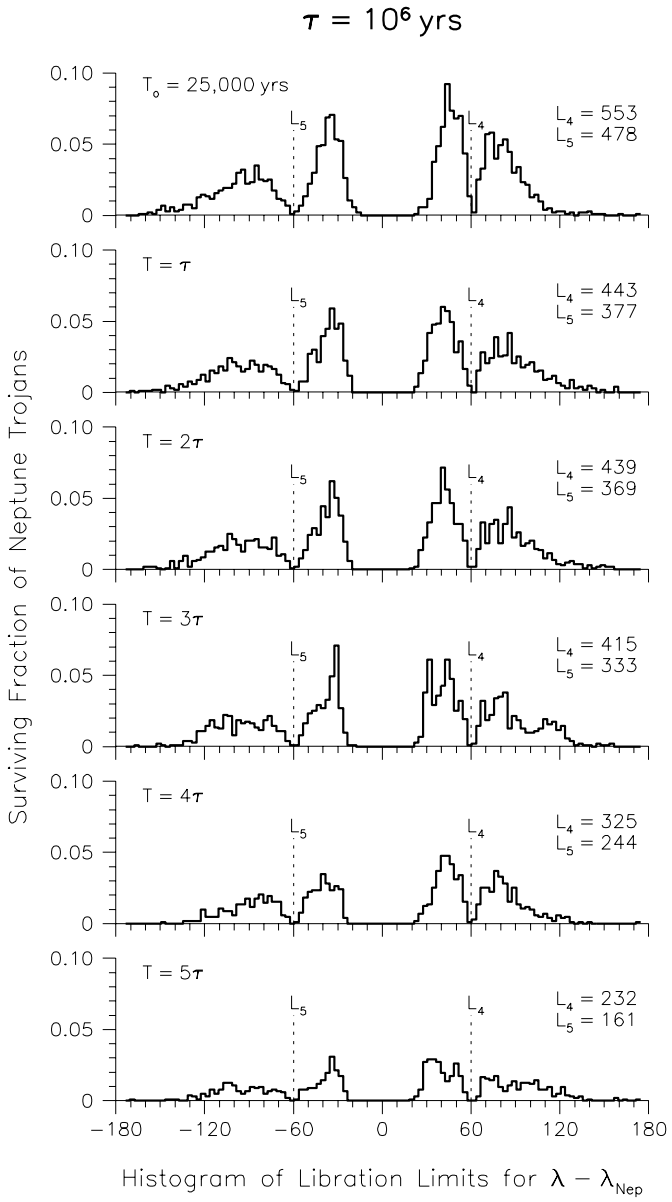

Figure 2: Survival of Neptune Trojans in a simulation with the four giant planets migrating with a characteristic time scale of $\tau = 10^6$ years. The six panels show minimum and maximum limits on libration of the critical argument, $\phi_{1:1}^{\rm NT} = \lambda - \lambda_{\rm Nep}$. The dashed lines at $\pm 60^\circ$ indicate the ideal locations of the leading L_4 and trailing L_5 Lagrange equilibrium points (for zero eccentricity). Each histogram gives the number of surviving Trojans in each bin as a fraction of the total population across all bins at the initial time $T_o = 25,000$ years. The top panel shows the initial distribution at time T_o. Each of the subsequent lower panels lists the output time in units of τ and the number of particles trapped in the L_4 and L_5 regions.

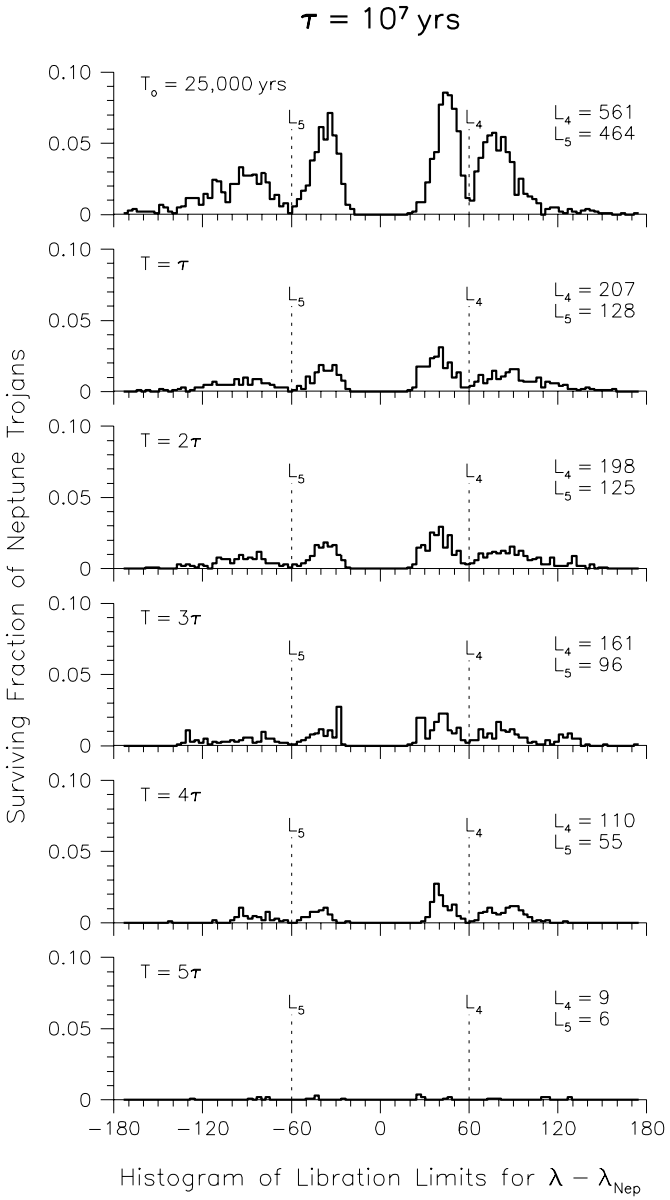

Figure 3: Similar to Fig. 2 but from a simulation with characteristic time scale 10 times slower, $\tau = 10^7$ years. All other initial conditions were identical to the simulations shown in Fig. 2. In this slow migration simulation nearly 99% of Neptune's initial Trojan companions are lost after 5τ.

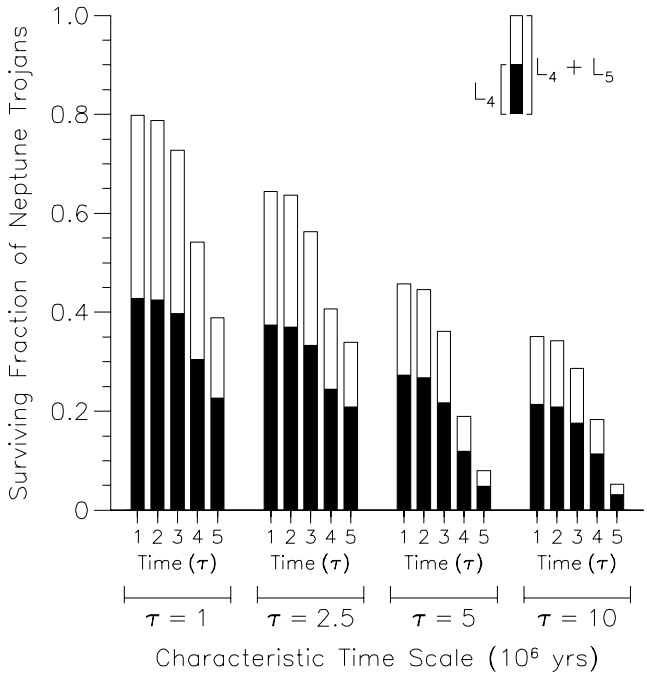

Figure 4: Histogram of the surviving fraction of Neptune Trojans as a function of time for four different characteristic migration time scales, τ, ranging from 10^6 to 10^7 years. In each case, time is expressed as integer multiples of τ up to 5τ. Solid and open bars indicate surviving fractions of Trojans in Neptune's leading L_4 and trailing L_5 regions, respectively. For each value of τ, simulations with identical initial conditions were run on four different types of processors, two Intel Xeons (1.7 and 2.4 GHz), a Digital Alpha EV6, and a Sun Sparc Ultra 5. The results shown in the histogram are a composite from all four simulations.

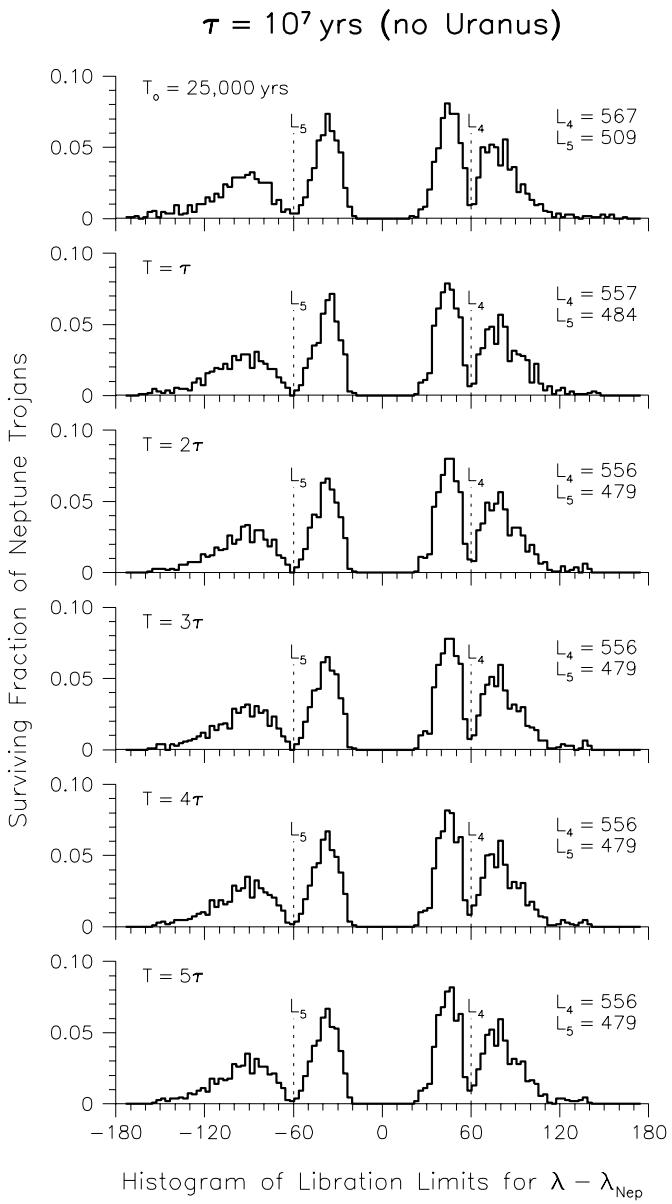

Figure 5: Similar to Fig. 2 ($\tau = 10^7$) but from a simulation that included Jupiter, Saturn, and Neptune, but not Uranus. Removing Uranus resulted in nearly full retention of Neptune Trojans up to a time of 5τ.

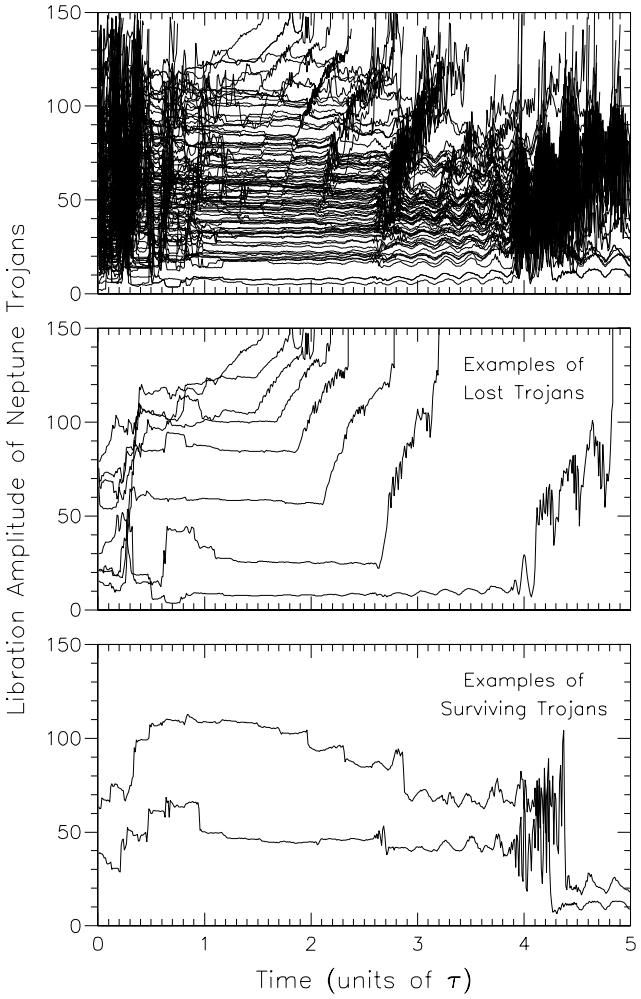

Figure 6: The libration amplitude of Neptune Trojans as a function of time expressed in units of τ for a simulation with $\tau = 5 \times 10^6$ years. Evolution of the general population is shown in the top panel. To avoid saturation only every fifth particle is plotted and libration amplitudes greater than 180° are not connected. After a time of τ, loss of Trojans is generally marked by cascading of particles out of resonance during a discrete number of prolonged events. Examples of Trojans lost during these episodes are shown in the middle panel. Trojans not lost by this process are still perturbed and can have their libration amplitudes decreased, as seen in the descending step-like appearance of the libration amplitudes of the survivors shown in the bottom panel.

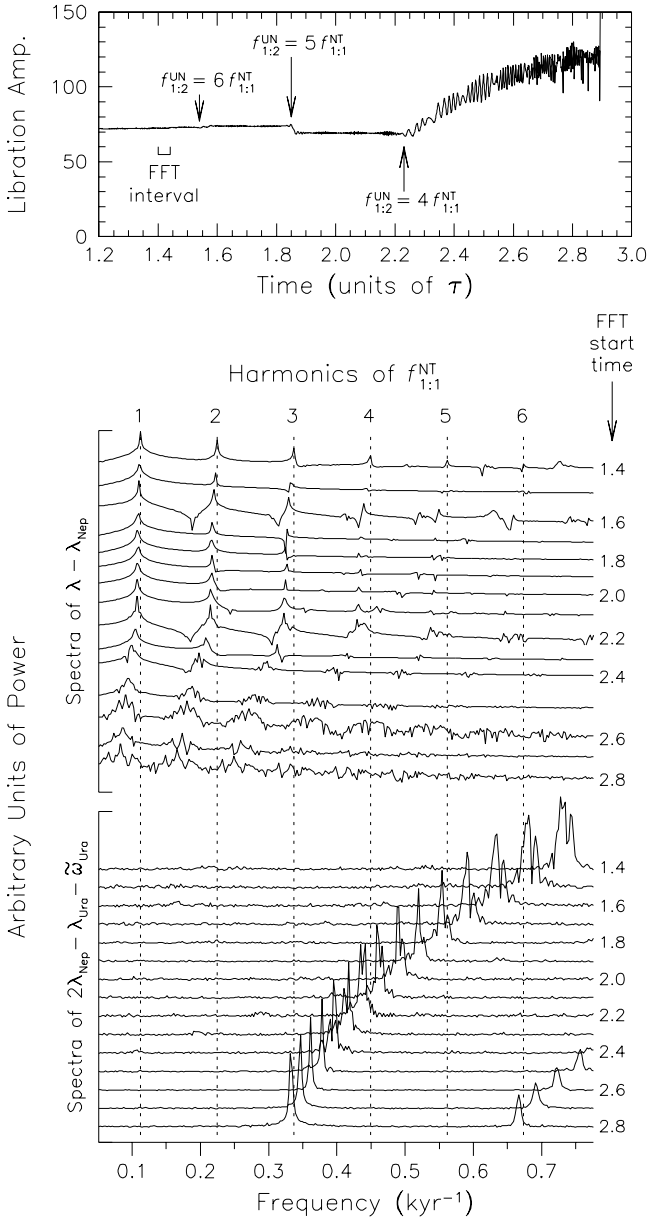

Figure 7: Evolution of the libration amplitude for one of the lost Trojans from a $\tau = 10^7$ year simulation is shown here at high resolution (top panel). A fast Fourier transform (FFT) was used to obtain power spectra of critical arguments for both the Neptune-Trojan 1:1 resonance ($\phi_{1:1}^{\rm NT} = \lambda - \lambda_{\rm Nep}$, middle panel) and the Uranus-Neptune 1:2 near-resonance ($\phi_{1:2}^{\rm UN} = 2\lambda_{\rm Nep} - \lambda_{\rm Ura} - \tilde{\omega}_{\rm Ura}$, bottom panel). Each FFT used 4096 points sampled every 100 years (see FFT interval bar), resulting in a Nyquist critical frequency (5 kyr^{-1}) well removed from the range shown here. The start times of the FFTs are indicated to the right of the spectra. Spectra of $\phi_{1:1}^{\rm NT}$ (middle panel) are shown in units of log power in order to simultaneously resolve the fundamental frequency ($f_{1:1}^{\rm NT}$) and its higher harmonics. The initial positions of the first six harmonics of $f_{1:1}^{\rm NT}$ are indicated by the dashed lines. As $f_{1:2}^{\rm UN}$ converges toward $f_{1:1}^{\rm NT}$ it overtakes the 6$^{\rm th}$ and then the 5$^{\rm th}$ harmonics of $f_{1:1}^{\rm NT}$. The Trojan particle experiences sudden changes in libration amplitude during these passages (indicated in top panel). At about $2.23\,\tau$ (see spectra taken at $2.2\,\tau$) the 4$^{\rm th}$ harmonic of $f_{1:1}^{\rm NT}$ becomes locked to $f_{1:2}^{\rm UN}$.

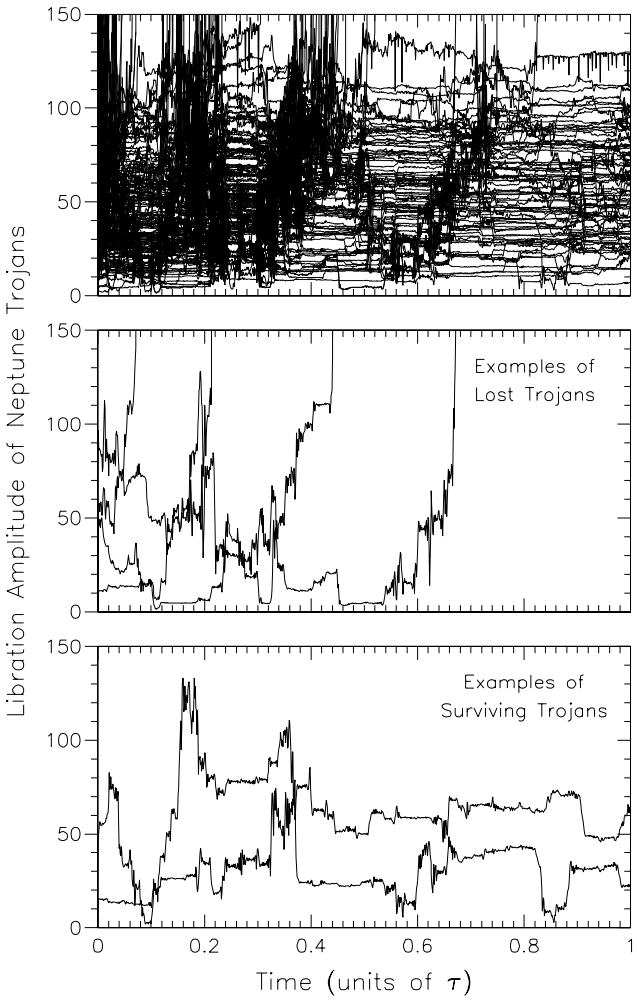

Figure 8: Similar to Fig. 6 except shown at higher temporal resolution for the period from time 0 to τ.

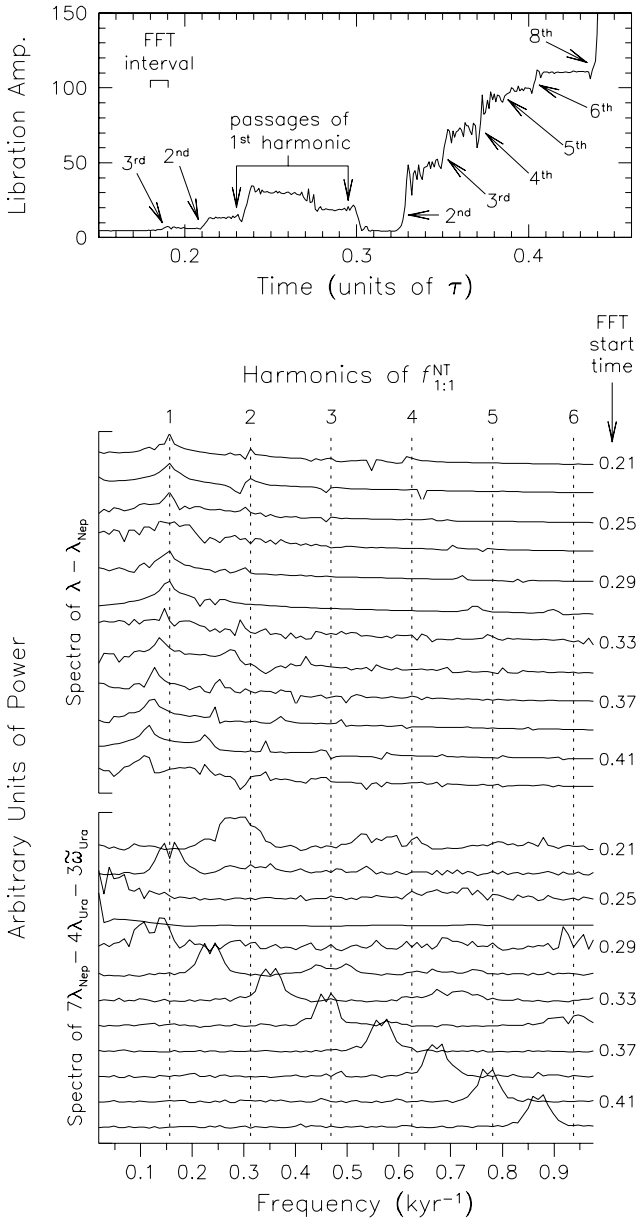

Figure 9: Similar to Fig. 7. The libration amplitude of one Trojan particle from Fig. 8 is shown at higher resolution (top panel). Power spectra of $\phi^{\rm NT}_{1:1}$ (middle panel, in log power) are compared with spectra of a critical argument for the 4:7 mean-motion resonance with Uranus ($\phi^{\rm UN}_{4:7} = 7\lambda_{\rm Nep} - 4\lambda_{\rm Ura} - 3\tilde{\omega}_{\rm Ura}$). Spectra were taken every 0.02τ (2×10^5 years) from 0.21 to 0.43τ (labeled to right of spectra). Each FFT used 1024 points sampled every 100 years, giving an FFT interval (indicated in top panel) of about 0.01τ. Note that dashed lines only indicate initial locations of the first six harmonics of $f^{\rm NT}_{1:1}$. By the later spectra, $f^{\rm NT}_{1:1}$ has slowed sufficiently to move the 8$^{\rm th}$ harmonic into the frame.

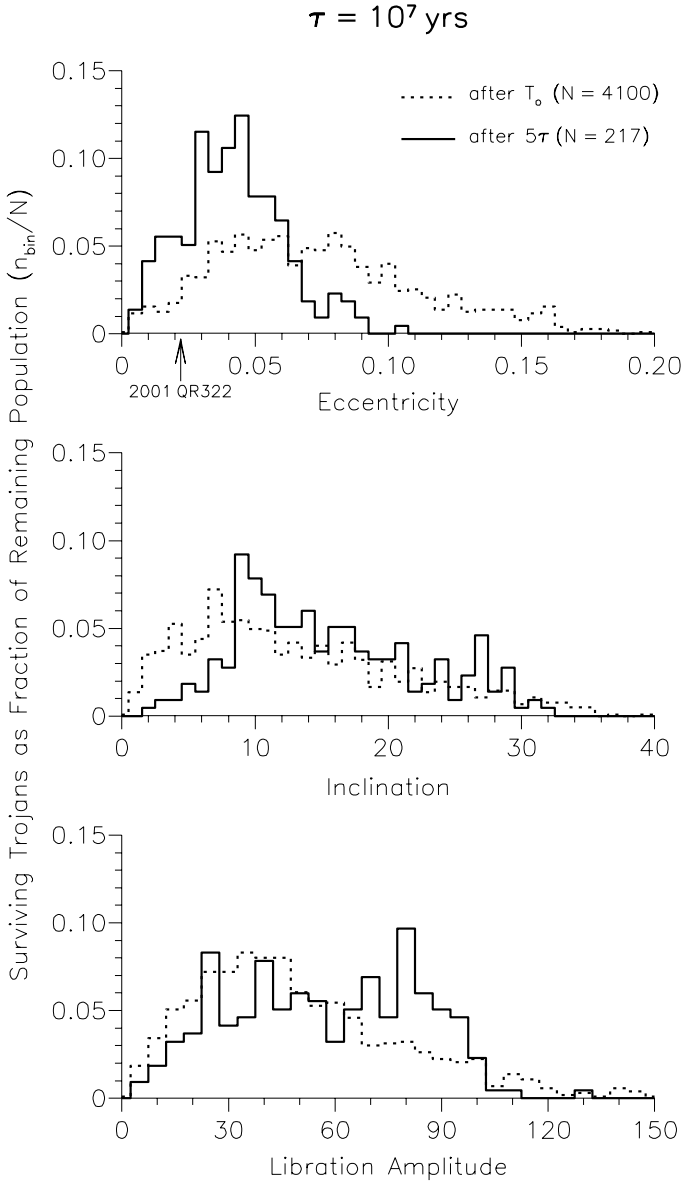

Figure 10: Histograms showing the distributions of eccentricity, inclination, and libration amplitude from the $\tau = 10^7$ year simulations. The dashed line indicates the initial distribution at $\mathsf{T}_\mathrm{o} = 25,000$ years and the solid line is the final distribution after 5τ. N indicates the number of Trojan particles remaining after T_o and 5τ. The orbital eccentricity of 2001 QR 322 is also indicated.

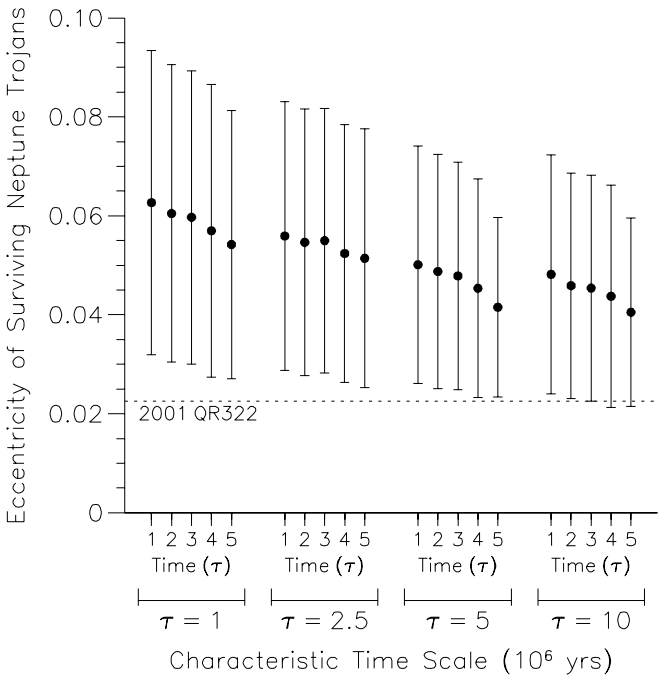

Figure 11: Distribution of orbital eccentricity of the surviving Neptune Trojans as a function of time for four different characteristic migration time scales, τ, ranging from 10^6 to 10^7 years. Points are the mean and error bars are one standard deviation. The orbital eccentricity of 2001 QR 322 is shown by the dashed line.